International Journal of Modern Physics E

SHELL MODEL FOR HEAVY NUCLEI AND ITS APPLICATION IN NUCLEAR ASTROPHYSICS

YANG SUN

Department of Physics and Joint Institute for Nuclear Astrophysics
University of Notre Dame, Notre Dame, Indiana 46556, USA
ysun@nd.edu

Received (received date)
Revised (revised date)

Performing shell model calculations for heavy nuclei is a long-standing problem in nuclear physics. The shell model truncation in the configuration space is an unavoidable step. The Projected Shell Model (PSM) truncates the space under the guidance of the deformed mean-field solutions. This implies that the PSM uses a novel and efficient way to bridge the two conventional methods: the deformed mean-field approximations, which are widely applied to heavy nuclei but able to describe the physics only in the intrinsic frame, and the spherical shell model diagonalization method, which is most fundamental but feasible only for small systems. We discuss the basic philosophy in construction of the PSM (or generally PSM-like) approach. Several examples from the PSM calculations are presented. Astrophysical applications are emphasized.

1. Introduction

The nuclear shell model is the most fundamental way of describing many-nucleon systems fully quantum mechanically. However, using the conventional shell model based on a spherical basis to study deformed, heavy nuclei is a very difficult task because of large dimensionality and its related problems. Even with today's computer power, the best standard shell-model diagonalization can be done only in the full pf-shell space, as for instance demonstrated by Caurier *et al.*[1], for which the dimension of the configuration space may already reach one billion. It seems impossible to apply this kind of shell model calculation to arbitrarily large systems.

In performing calculations for a many-nucleon system, one should choose a proper shell-model basis to start with. While in principle, it does not matter how to prepare a model basis, it is important in practice to use the most efficient one. In this regard, we recognize the fact that except for a few lying in the vicinity of shell closures, most nuclei in the nuclear chart are deformed. This suggests strongly for shell model calculations to use a *deformed* basis to incorporate correlations in large systems efficiently. However, a deformed basis is associated with breaking of rotational symmetry and angular momentum in that basis is no longer a good quantum number. Although in some cases physics may be discussed in deformed bases at-

tached to the system (intrinsic frames), the broken rotational symmetry should, at least in principle, be restored by angular-momentum-projection, which corresponds to a transformation from the intrinsic frame back to the laboratory frame. Shell model diagonalization is then carried out in the projected basis defined in the laboratory frame. This is the scheme that the Projected Shell Model[2] is based on. It may represent a group of practical methods that allow one to perform shell model diagonalization calculations for deformed, heavy nuclei.

In recent years, strong demand for a shell-model treatment for nuclei arises also from nuclear astrophysics. Since heavy elements are made in stellar evolution and explosions, nuclear physics and, in particular, nuclear structure far from stability, enters into the stellar modeling in a crucial way (see the recent review[3] by Aprahamian, Langanke, and Wiescher). The nucleosynthesis and the correlated energy generation are not completely understood, and the origin of elements in the cosmos remains one of the unsolved physics puzzles. Nuclear shell-models can generate well-defined wave functions, allowing one to compute, without further approximations as often assumed in the mean-field methods, quantities such as transition probabilities, spectroscopic factors, and β-decay and electron-capture rates for both ground state and excited states. These quantities provide valuable structure information for nuclear astrophysics. Indeed, in their example[4], Langanke and Martínez-Pinedo has demonstrated that shell-model calculations could significantly modify the results of nuclear astrophysics.

2. The projected shell model

In performing shell-model-type calculations for large nuclear systems, the central issue has been how to truncate the shell-model space efficiently. It corresponds to a rearrangement of the configuration space to decouple the most important part from the rest of the space. There are many different schemes of truncating a shell-model space[5,6,7,8,9,10]. Although these schemes differ very much in details in the way of building the model bases and/or choosing effective interactions, they share the common character that the model space is first constructed by some physical guidance. The so obtained model space contain the most significant configurations, each of which can be a very complicated combination in terms of the spherical shell-model basis states. In this way, the basis dimension can be significantly reduced and the final diagonalization is carried out in a much smaller space, thus making a shell-model calculation for heavy nuclei possible.

The present article reviews a particular truncation scheme implemented in the Projected Shell Model (PSM)[2]. One friendly feature of the PSM is its simplicity. It starts with the deformed Nilsson model combined by a BCS calculation to generate quasiparticle (qp) states. The Nilsson model[11] is one of the most successful single-particle models that has been carefully tested for different mass regions. In a PSM calculation, the shell model truncation is first achieved within the qp states with respect to the deformed Nilsson + BCS qp vacuum $|0\rangle$; then the broken rotational

symmetry (also broken particle-number and parity conservation, if necessary) is restored for these states by standard projection techniques[12] to form a shell model basis in the laboratory frame; finally a two-body Hamiltonian is diagonalized in this basis. The truncation obtained in this way is very efficient. For example, for excited rotational bands in a deformed, heavy nucleus (see examples below), quite satisfactory results can be obtained by a diagonalization within a dimension smaller than 100. In short, the PSM starts with deformed single particle states generated by (in principle any) mean-field solutions on one side, and performs a shell model diagonalization like a spherical shell model (but in a much smaller space) on the other. Such an approach lies conceptually between the two conventional methods: deformed mean-field model and spherical shell model, thus naturally bridges the two methods that have coexisted but rarely have any connections.

The Nilsson + BCS calculation defines a set of deformed qp states (with $a^\dagger_\nu$ and $a^\dagger_\pi$ being the creation operator for neutrons and protons, respectively) with respect to the qp vacuum $|0\rangle$. The PSM basis is constructed in the multi-qp states with the following forms

- e-e: $\{|0\rangle, a^\dagger_\nu a^\dagger_\nu|0\rangle, a^\dagger_\pi a^\dagger_\pi|0\rangle, a^\dagger_\nu a^\dagger_\nu a^\dagger_\pi a^\dagger_\pi|0\rangle, a^\dagger_\nu a^\dagger_\nu a^\dagger_\nu a^\dagger_\nu|0\rangle, a^\dagger_\pi a^\dagger_\pi a^\dagger_\pi a^\dagger_\pi|0\rangle, \ldots\}$
- o-o: $\{a^\dagger_\nu a^\dagger_\pi|0\rangle, a^\dagger_\nu a^\dagger_\nu a^\dagger_\nu a^\dagger_\pi|0\rangle, a^\dagger_\nu a^\dagger_\pi a^\dagger_\pi a^\dagger_\pi|0\rangle, a^\dagger_\nu a^\dagger_\nu a^\dagger_\nu a^\dagger_\pi a^\dagger_\pi a^\dagger_\pi|0\rangle, \ldots\}$
- odd-ν: $\{a^\dagger_\nu|0\rangle, a^\dagger_\nu a^\dagger_\nu a^\dagger_\nu|0\rangle, a^\dagger_\nu a^\dagger_\pi a^\dagger_\pi|0\rangle, a^\dagger_\nu a^\dagger_\nu a^\dagger_\nu a^\dagger_\pi a^\dagger_\pi|0\rangle, \ldots\}$
- odd-π: $\{a^\dagger_\pi|0\rangle, a^\dagger_\nu a^\dagger_\nu a^\dagger_\pi|0\rangle, a^\dagger_\pi a^\dagger_\pi a^\dagger_\pi|0\rangle, a^\dagger_\nu a^\dagger_\nu a^\dagger_\pi a^\dagger_\pi a^\dagger_\pi|0\rangle, \ldots\}$

for even-even, odd-odd, odd-neutron, and odd-proton nuclei, respectively. A general term in above expressions may be written as $|\phi_\kappa\rangle$, with κ denoting all the quantum numbers, such as the Nilsson quantum numbers, necessary to specify that term. The angular-momentum-projected multi-qp states are thus *building blocks* in the PSM wavefunction, which can be generally written as

$$|\psi^{I,\sigma}_M\rangle = \sum_{\kappa,K\leq I} f^{I,\sigma}_\kappa \hat{P}^I_{MK}|\phi_\kappa\rangle = \sum_\kappa f^{I,\sigma}_\kappa \hat{P}^I_{MK_\kappa}|\phi_\kappa\rangle. \tag{1}$$

The index σ labels states with same angular momentum and κ the basis states. $\hat{P}^I_{MK}$ is the angular-momentum-projection operator[12] and the coefficients $f^{I,\sigma}_\kappa$ are weights of the basis states.

The weights $f^{I,\sigma}_\kappa$ are determined by diagonalization of the Hamiltonian in the spaces spanned for various nuclear systems as listed above, which leads to the eigenvalue equation (for a given I)

$$\sum_{\kappa'} (H_{\kappa\kappa'} - E_\sigma N_{\kappa\kappa'})\, f^\sigma_{\kappa'} = 0. \tag{2}$$

The Hamiltonian and the norm matrix elements in Eq. (2) are given as

$$H_{\kappa\kappa'} = \langle\phi_\kappa|\hat{H}\hat{P}^I_{K_\kappa K'_{\kappa'}}|\phi_{\kappa'}\rangle, \qquad N_{\kappa\kappa'} = \langle\phi_\kappa|\hat{P}^I_{K_\kappa K'_{\kappa'}}|\phi_{\kappa'}\rangle. \tag{3}$$

Angular-momentum-projection on a multi-qp state $|\phi_\kappa\rangle$ with a sequence of I generates a band. One may define the rotational energy of a band (band energy) using

the expectation values of the Hamiltonian with respect to the projected $|\phi_\kappa\rangle$

$$E^I_\kappa = \frac{H_{\kappa\kappa}}{N_{\kappa\kappa}} = \frac{\langle\phi_\kappa|\hat{H}\hat{P}^I_{K_\kappa K_\kappa}|\phi_\kappa\rangle}{\langle\phi_\kappa|\hat{P}^I_{K_\kappa K_\kappa}|\phi_\kappa\rangle}. \tag{4}$$

The central technical issue is how to compute the matrix elements, such as those in Eq. (3), in the projected states. This question applies generally to any models utilizing angular momentum projection. Following the pioneering work of Hara and Iwasaki[13], a systematic derivation has been obtained for any one and two-body operators (of separable forces) with an arbitrary number of quasi-particles in the projected states[2,14]. In principle, the projected multi-qp basis recovers the full shell model space *if* all the quasi-particles in the valence space were considered in building the multi-qp states. However, the advantage of working with a deformed basis is that the selection of only a few quasi-particles near the Fermi surface is already sufficient to construct a good shell model space. The rest can simply be truncated out.

In a usual approximation with independent quasiparticle motion (mean-field solutions), the energy for a multi-qp state is simply taken as the sum of those of single quasiparticles. This is the dominant term. The present theory modifies this quantity in the following two steps. First, the band energy defined in Eq. (4) introduces the correction brought by angular momentum projection and the two-body interactions, which accounts for the couplings between the rotating body and the quasiparticles in a quantum-mechanical way. Second, the corresponding rotational states are mixed in the subsequent procedure of solving the eigenvalue equation (2). The energies are thus further modified by the configuration mixing.

If the deformed states have an axial symmetry, each of the basis states in (1), the projected $|\phi_\kappa\rangle$, is a K-state. For example, an n-qp configuration gives rise to a multiplet of 2^{n-1} states, with the total K expressed by $K = |K_1 \pm K_2 \pm \cdots \pm K_n|$, where K_i is for an individual neutron or proton. In this case, shell model diagonalization, i.e. solving the eigenvalue equation (2), is completely equivalent to a K-mixing. The amount of the mixing can be obtained from the resulting wavefunctions.

The above discussion is independent of the choice of the two-body interactions in the Hamiltonian. In practical calculations, the PSM uses the pairing plus quadrupole-quadrupole Hamiltonian (that has been known to be essential in nuclear structure calculations[15,16]) with inclusion of the quadrupole-pairing term

$$\hat{H} = \hat{H}_0 - \frac{1}{2}\chi\sum_\mu \hat{Q}^\dagger_\mu\hat{Q}_\mu - G_M\hat{P}^\dagger\hat{P} - G_Q\sum_\mu \hat{P}^\dagger_\mu\hat{P}_\mu. \tag{5}$$

The strength of the quadrupole-quadrupole force χ is determined in such a way that it has a self-consistent relation with the quadrupole deformation ε_2. The monopole-pairing force constants G_M are

$$G_M = \left[G_1 \mp G_2\tfrac{N-Z}{A}\right]\ A^{-1}, \tag{6}$$

with "−" for neutrons and "+" for protons, which reproduces the observed odd–even mass differences in a given mass region if G_1 and G_2 are properly chosen. Finally, the strength G_Q for quadrupole pairing is simply assumed to be proportional to G_M, with a proportionality constant in the range of 0.14 to 0.20, as commonly used in the PSM calculations[2].

3. Examples

In this section, we show several examples from the recent PSM calculations. These include a light nucleus ^{48}Cr for which a full diagonalization of the pf-shell spherical shell model is available, a well-deformed nucleus ^{178}Hf in the heavy mass region with the well-known 31-year isomer, and a gateway nucleus ^{254}No to the superheavy "island of stability".

3.1. ^{48}*Cr: A benchmark for models of pf-shell rotors*

^{48}Cr is a light nucleus for which an exact shell model diagonalization in the pf-shell model space and a mean-field analysis have been performed[17]. Though light, this nucleus exhibits remarkable high-spin phenomena usually observed in heavy nuclei: large deformation, typical rotational spectrum, and the backbending phenomenon in which the regular rotational band is disturbed by a sudden irregularity at a certain spin. In the PSM calculations[18] for ^{48}Cr, three major shells (N = 1, 2, 3) are used for both neutrons and protons. The shell model space is truncated at the deformation $\varepsilon_2 = 0.25$.

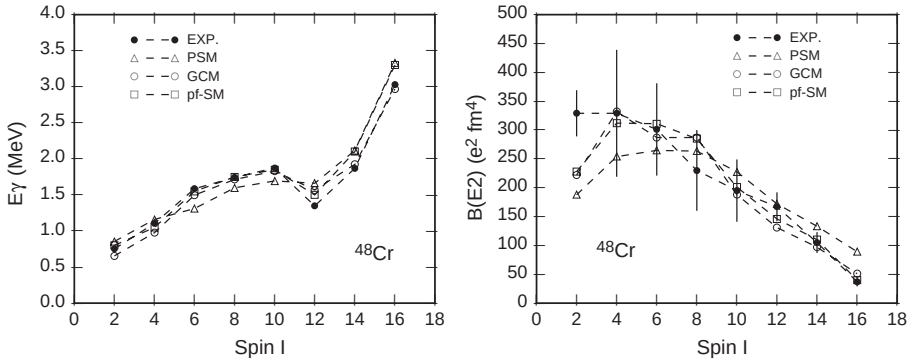

Fig. 1. Left panel: γ-ray energies $E_\gamma = E(I) - E(I-2)$ in ^{48}Cr as functions of spin. Right panel: B(E2) values as functions of spin. These figures are redrawn from Figs. 1 and 2 of Ref.[18].

In the left panel of Fig. 1, the PSM result for γ-ray energy along the yrast band, together with that of the pf-shell model (pf-SM) reported in Ref.[17], and that

of the Generator Coordinate Method (GCM)[18], are compared with the experimental data. One sees that the four curves are bunched together over the entire spin region, indicating an excellent agreement of the three calculations with each other, and with the data. The sudden drop in E_γ occurring around spin $I = 10$ and 12 corresponds to the backbending in the yrast band of ^{48}Cr. In the right panel of Fig. 1, three theoretical results for B(E2) are compared with the data. All the three calculations use the same effective charges (0.5e for neutrons and 1.5e for protons). Again, one sees that the theoretical descriptions agree not only with each other but also with the data quite well. The B(E2) values decrease monotonously after spin $I = 6$ (where the first band crossing takes place in the PSM). This implies a monotonous decrease of the intrinsic Q-moment as a function of spin, reaching finally the spherical regime at higher spins. This implies also that the final results of a shell model calculation do not depend on choice of the basis (either spherical ($\varepsilon_2 = 0$) or deformed ($\varepsilon_2 = 0.25$)); A spherical shell model can describe states with large deformation (low-spin states in Fig. 1) and a (projected) deformed shell model can describe states having spherical properties (high-spin states in Fig. 1).

The results shown in Fig. 1 suggest that the PSM is an efficient shell model truncation scheme that reproduces the data with the similar quality as the large-scale pf-SM. To compare with the one-major-shell shell model[17], the valence space in the PSM is much larger (three major shells) yet the shell-model basis is much smaller (< 100). An obvious advantage of the PSM is that because it works in a much smaller basis with the configurations having a clear physics meaning, the PSM is able to extract the undergoing physics easily. In another PSM calculation[19] for the super-deformed band in ^{36}Ar, the same conclusion was drawn. The PSM reproduces the data in a much simpler way and yields a similar quality in the results as those of the large-scale shell model[20].

3.2. ^{178}*Hf: A deformed heavy nucleus with a long-lived isomer*

Long-lived isomers - excited nuclear states with inhibited electromagnetic decay - may be considered to offer a form of energy storage[21,22]. The possibility to trigger the decay by the application of external electromagnetic radiation has attracted much interest and potentially could lead to the controlled release of nuclear energy[23]. The significantly high energy of the ^{178}Hf isomer leads to the expectation of a lower triggering threshold, on account of the higher level density. The high isomer energy (~ 2.5 MeV) and long half-life (31 years) in ^{178}Hf also leads to greater potential with regard to the utility of triggered energy release. In determining the favorable conditions for triggering γ-ray emission from the isomer, it is necessary to have information on the structure of possible gateway states, as well as possible paths of electromagnetic transitions to and from these states. Experimentally, only a few states close to the ^{178}Hf isomer have been observed[24,25].

In the PSM calculation[26] for ^{178}Hf, the model basis is built with the deformation parameters $\varepsilon_2 = 0.251$ and $\varepsilon_4 = 0.056$. The valence space includes three major shells

(N = 4, 5, and 6 for neutrons and N = 3, 4, and 5 for protons). Fig. 2 shows the calculated energy levels in ^{178}Hf, compared with the known data[24]. Satisfactory agreement is achieved for most of the states, except that for the bandhead of the first 8^- band and the 14^- band, the theoretical values are too low. The leading structure of each band can be read from the wave functions. We found that

- the 6^+ band has a 2-qp structure $\{\nu[512]\frac{5}{2}^- \oplus \nu[514]\frac{7}{2}^-\}$,
- the 16^+ band has a 4-qp structure $\{\nu[514]\frac{7}{2}^- \oplus \nu[624]\frac{9}{2}^+ \oplus \pi[404]\frac{7}{2}^+ \oplus \pi[514]\frac{9}{2}^-\}$,
- the first (lower) 8^- band has a 2-qp structure $\{\nu[514]\frac{7}{2}^- \oplus \nu[624]\frac{9}{2}^+\}$,
- the second (higher) 8^- band has a 2-qp structure $\{\pi[404]\frac{7}{2}^+ \oplus \pi[514]\frac{9}{2}^-\}$,
- and the 14^- band has a 4-qp structure $\{\nu[512]\frac{5}{2}^- \oplus \nu[514]\frac{7}{2}^- \oplus \pi[404]\frac{7}{2}^+ \oplus \pi[514]\frac{9}{2}^-\}$.

These states, together with many other states (not shown in Fig. 2) obtained from the same diagonalization, form a complete spectrum including the high-K isomeric states and candidate gateway states.

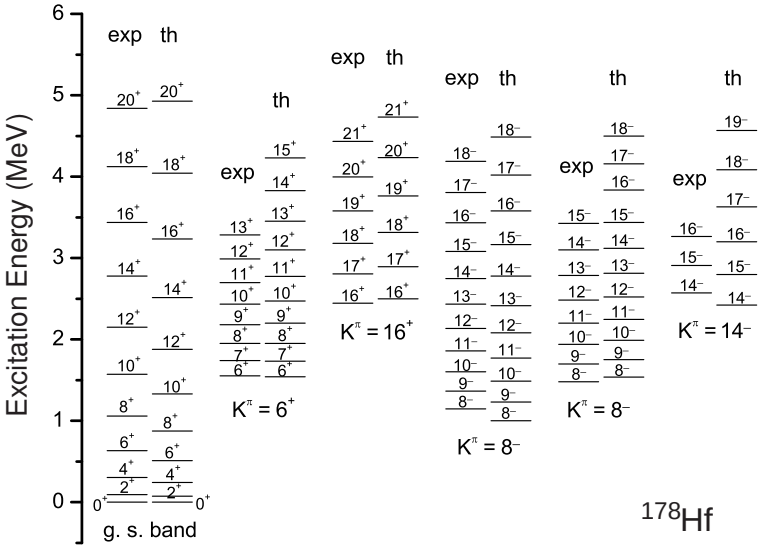

Fig. 2. Comparison of calculated energy levels in ^{178}Hf with known data[24]. This figure is adopted from Ref.[26].

This example has demonstrated that the PSM can be an appropriate nuclear structure theory for studying high-spin isomers and associated excitations, including potential gateway states for triggering the isomer decay. Since the diagonalization mixes the K-states, the resulting wavefunctions contain valuable information on K-mixing. One is thus able to use the wavefunctions to calculate the inter-band

transitions and to analyze the degree of K-mixing.

3.3. ^{254}*No: A gateway nucleus to the superheavy "island of stability"*

One key question in our understanding of the chemical building blocks of the Universe is what is the heaviest element that can exist. Intimately linked to this question is the problem in nuclear physics of the shell stabilization of superheavy nuclei. In a simplistic model of the nucleus, the repulsive force between more than 100 positively charged protons is sufficient to overcome the attractive strong nuclear force and induce the nucleus to fission. However, protons and neutrons fall into shell structures which, in analogy to the enhanced stability of noble gases, give extra binding to nuclei in a closed shell configuration. The largest binding comes from a coincidence of closed shells for both protons and neutrons, as in ^{16}O (Z = N = 8), ^{40}Ca (Z = N = 20), ^{132}Sn (Z = 50, N = 82) and ^{208}Pb (Z = 82, N = 126).

What is the next closed shell for protons, i.e. where is a region of long-lived, or even stable, superheavy elements beyond the actinides? Modern theoretical calculations disagree on the size and position of the island of stability. For the possible sources that lead to the disagreement, one may question the single-particle levels in those calculations. One accessible way to gain information on these states with today's experimental situation is to study the high-K isomer states in Z $\approx$ 100 nuclei. These isomer states are highly significant as their structure is very sensitive to single-particle levels. Recently, Xu *et al.*[27] have suggested that the existence of the isomer states can result in increased survival probabilities of superheavy nuclei.

The PSM is employed to study the structure of high-K isomer states in ^{254}No and the obtained results are compared with data from the recent experiment by Herzberg *et al.*[28]. In the PSM calculation, three major shells are activated for both neutrons and protons (N = 5, 6, 7 for neutrons and 4, 5, 6 for protons). The deformed basis for the ^{254}No calculation is constructed with $\varepsilon_2 = 0.25$. For the pairing interaction strengths in the Hamiltonian, we take $G_1 = 21.24$, $G_2 = 13.13$, and $G_Q = 0.14$.

We first compare the theoretical results with the known ^{254}No data[28] for the yrast band. As can be seen in the left panel of Fig. 3, the theory has well reproduced the data. The current data ends at $I = 20$ where the rotational alignment process is about to start. After that spin, the theory predicts a weak up-bending in moment of inertia. In the right panel of Fig. 3, band energies (as defined in Eq. (4)) of several important configurations are plotted to understand why this up-bending occurs. While the 0-qp band lies low in energy till $I = 20$, the low-K 2-qp band ($K^\pi = 1^+, \nu[743]\frac{7}{2}^- \oplus \nu[734]\frac{9}{2}^-$) crosses the 0-qp band at $I = 22$ and becomes the lowest one for the next spin states. At $I = 30$, the 2-qp band is crossed by the low-K 4-qp band ($K^\pi = 0^+, \nu[743]\frac{7}{2}^- \oplus \nu[734]\frac{9}{2}^- \oplus \pi[633]\frac{7}{2}^+ \oplus \pi[624]\frac{9}{2}^+$), and the latter becomes the lowest one for the high-spin region. The predicted up-bending effect centering at $I = 26$ in the left panel is thus attributed to the two successive

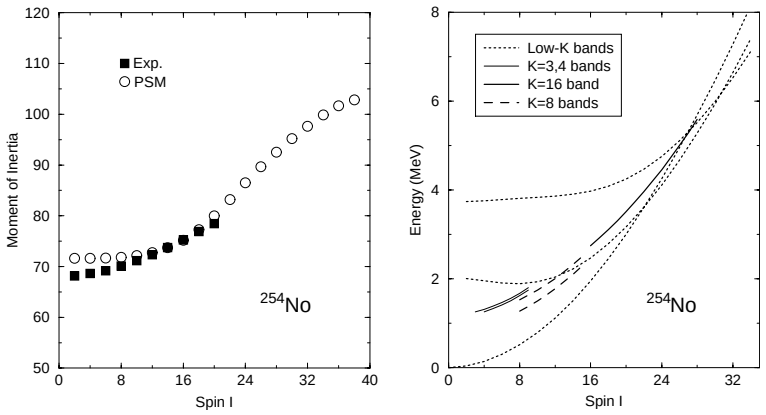

Fig. 3. Left panel: Comparison of the predicted yrast band in ^{254}No with known data[28]. Right panel: Selected band energies before band-mixing, which represent the most important configurations.

band crossings with presence of strong band interactions.

Among the high-K 2-qp states, the one with $K^\pi = 8^-$ coupled from two neutrons ($\nu[624]\frac{7}{2}^+ \oplus \nu[734]\frac{9}{2}^-$) is found to be the lowest in energy. The next lowest 8^- state is from two protons ($\pi[514]\frac{7}{2}^- \oplus \pi[624]\frac{9}{2}^+$). These two 8^- bands are found well-separated from the rest 2-qp bands. The predicted bandhead energies for the two 8^- bands are 1.266 and 1.516 MeV, respectively, very close to the experimental 8^- isomer at 1.293 MeV [28].

The combination of these two 2-qp 8^- states can give a 4-qp state with the highest possible K. This $K^\pi = 16^+$ state thus has the configuration ($\nu[624]\frac{7}{2}^+ \oplus \nu[734]\frac{9}{2}^- \oplus \pi[514]\frac{7}{2}^- \oplus \pi[624]\frac{9}{2}^+$). This is the lowest 4-qp band found in the calculation, which is again well-separated (in energy and in K) from other 4-qp states. Although the bandhead state ($I = 16$) already lies in a dense region, its unique K quantum number hinders its decay. The predicted bandhead energy for the 16^+ band is 2.750 MeV. Very likely, this is the structure for the experimental 184-μs isomer[28].

4. Application in nuclear astrophysics

Nuclear structure input is important, and sometimes crucial, for nuclear astrophysics. For example, an isomeric state can communicate with its ground state through thermal excitations in hot astrophysical environments. This could alter the elemental abundances produced in nucleosynthesis. We are just beginning[22] to look at the impact that isomers have on various nucleosynthesis processes such as the rapid proton capture process thought to take place on the accretion disks of binary neutron stars. Shell model calculations for understanding the isomer structures and the decay rates are very much desired for this study.

4.1. *Nuclear shape isomers in the rp-process path*

It has been suggested that in x-ray binaries, nuclei are synthesized via the rapid proton capture process (rp process)[29], a sequence of proton captures and β-decays responsible for the burning of hydrogen into heavier elements. The rp process proceeds through an exotic mass region with N $\approx$ Z, where the nuclei exhibit unusual structure properties. One of those is the coexistence of two or more stable shapes in a nucleus at comparable excitation energies in nuclei with A $\approx$ 70 - 80. The nuclear shapes include, among others, prolate and oblate deformations. In an even-even nucleus, the lowest state with a prolate or an oblate shape has quantum numbers $I^\pi = 0^+$. An excited 0^+ state may decay to the ground 0^+ state via an electric monopole (E0) transition. For lower excitation energies, the E0 transition is usually slow, and thus the excited 0^+ state becomes a "shape isomer".

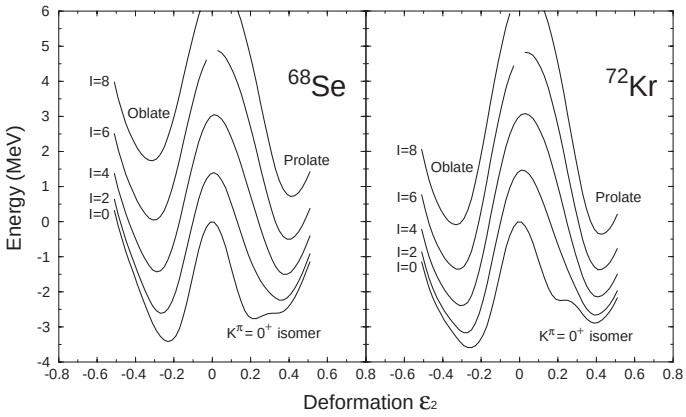

Fig. 4. Energy surfaces for various spin states in ^{68}Se and ^{72}Kr as a function of deformation variable ε_2. This figure is adopted from Ref.[30].

Fig. 4 shows calculated total energies[30] as a function of the deformation variable ε_2 for different spin states in ^{68}Se and ^{72}Kr. The configuration space and the interaction strengths in the Hamiltonian can be found in the previous calculations for the same mass region[31]. Under these calculation conditions, it is found that in both nuclei, the ground state takes an oblate shape with $\varepsilon_2 \approx -0.25$. As spin increases, the oblate minimum moves gradually to $\varepsilon_2 \approx -0.3$. Another local minimum with a prolate shape ($\varepsilon_2 \approx 0.4$) is found to be 1.1 MeV (^{68}Se) and 0.7 MeV (^{72}Kr) high in excitation. Bouchez *et al.*[32] observed the 671 keV shape-isomer in ^{72}Kr with half-life $\tau = 38 \pm 3$ ns. The one in ^{68}Se is our prediction[30], awaiting experimental confirmation. Similar isomer states have also been calculated by Kaneko, Hasegawa, and Mizusaki[33].

Since the ground states of ^{73}Rb and ^{69}Br are bound with respect to the isomers

in ^{72}Kr and ^{68}Se, proton capture on these isomers may lead to additional strong feeding of the ^{73}Rb$(p,\gamma)^{74}$Sr and ^{69}Br$(p,\gamma)^{70}$Kr reactions. However, whether these branches have any significance depends on the associated nuclear structure parameters, such as

- how strong is the feeding of the isomer states?
- what is the lifetime of the isomer with respect to γ-decay and also to β-decay?
- what are the lifetimes of the proton unbound ^{69}Br and ^{73}Rb isotopes in comparison to the proton capture on these states?

The lifetime of the isomeric states must be sufficiently long to allow proton capture to take place. No information is presently available about the lifetime of the ^{68}Se isomer. Based on Hauser-Feshbach estimates[29] the lifetime against proton capture is in the range of $\approx$ 100 ns to 10 μs, depending on the density in the environment. Considering the uncertainties in the present estimates a fair fraction may be leaking out of the ^{68}Se, ^{72}Kr equilibrium abundances towards higher masses.

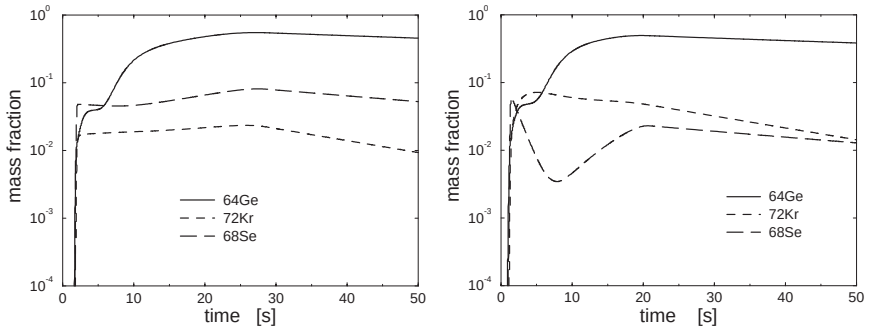

Fig. 5. Mass fractions in the x-ray burst model with two extreme cases. This figure is adopted from Ref.[30].

While it is likely that equilibrium is ensued between all these configurations within the presently given experimental limits a considerable flow towards higher masses through the isomer branch cannot be excluded. Figure 5 shows the comparison between the two extreme possibilities for the reaction sequence calculated in the framework of a multi-mass-zone x-ray burst model[34]. The left panel shows the mass fractions of ^{64}Ge, ^{68}Se, and ^{72}Kr as a function of time neglecting any possible isomer contribution to the flow. The right panel shows the results from the same model assuming full reaction flow through the isomeric states in ^{68}Se and ^{72}Kr rather than through the respective ground states. The main differences in ^{68}Se and ^{72}Kr mass fractions are due to rapid initial depletion in the early cooling phase of the burst. This initial decline is compensated subsequently by decay feeding from the long lived ^{64}Ge abundance. The results of our model calculations are based

on upper and lower limit assumptions about the role of the shape isomer states. Improved calculations would require better nuclear structure data to identify more stringent limits on the associated reaction and decay rate predictions.

4.2. *Weak interaction rates*

The knowledge on weak interaction processes is another important ingredient for resolving astrophysical problems. The decisive role played by the Gamow-Teller (GT) transitions has since long been recognized. It has been suggested that the nuclear shell model is the most preferable method for GT transition calculations. This has recently been emphasized by Langanke and Martínez-Pinedo[4].

For a theoretical model employed in GT transition calculations, it is generally required that the model can reproduce a wide range of structure properties of relevant nuclei. It has been shown that the conventional shell-model diagonalization method is indeed capable of performing such calculations. For example, Wildenthal and Brown[35,36] obtained nuclear wave functions in the full *sd*-shell model space, which were successfully applied to calculation of GT rates in the *sd* shell nuclei[37]. Langanke and Martínez-Pinedo[38] made the shell-model GT rates available also for the *pf* shell nuclei. Still, these sophisticated calculations are tractable only for nuclei up to the mass-60 region, and cannot be applied to heavier nuclei which play important roles in the nuclear processes in massive stars.

In GT transition calculations for heavy nuclei, the PSM wavefunctions can be used. Here, we wish to list a few attractive features in this approach, which may be relevant for future astrophysical applications.

- Because of the way the PSM constructs its basis, the dimension of the model space is small (usually in the range of $10^2 - 10^4$). With this size of basis, a state-by-state evaluation of GT transition rates is computationally feasible. This feature is important because in stellar environments with finite temperatures, the usual situation is that the thermal population of excited states in a parent nucleus sets up connections to many states in a daughter by the GT operator. Our current knowledge on GT transitions from excited nuclear states is however very poor, and in many cases, it must rely on theoretical calculations.
- The PSM is a multi-shell shell model. This feature is desired for the processes in which forbidden transitions are dominated by the collective response of nuclei. The corresponding calculations must involve nuclear transitions between different harmonic-oscillator shells, and thus require a shell model working in a multi-shell model space.
- The existence of isomeric states in nuclei could alter significantly the elemental abundances produced in nucleosynthesis. There are cases in which an isomer of sufficiently long lifetime can change the paths of reactions taking place and lead to a different set of elemental abundances. We have seen in above discussions that the PSM is indeed capable of describing the detailed structure of isomeric states.

Very recently, we have developed a method[39] for calculation of GT transition rates based on the PSM. We expect that this method can generally be applied to the fields where weak interaction processes take place in nuclear systems. In particular, one may find interesting applications to cases where a laboratory measurement for certain weak interaction rates is difficult and where the conventional shell model calculations are not feasible. Potential applications in nuclear astrophysics are calculations of β-decay rates for the r-process and the rp-process nucleosynthesis, and electron-capture rates for the core collapse supernova modelling.

5. Summary

It has been desired that one enjoys advanced shell model diagonalization methods while pushing the calculations to heavy nuclear systems. However, most of the updated spherical shell model calculations are severely limited in the fp-shell nuclei or nuclei in the vicinity of shell closures. We have shown that the Projected Shell Model may be an efficient truncation scheme for a shell model solution. While it takes the advantages from the mean-filed results, the PSM also contains the shell model character that it performs configuration mixing in a truncated basis. We have shown through the calculation for ^{48}Cr that the PSM results are comparable with those obtained by the large-scale shell model calculations based on the spherical basis. We have also presented examples for heavy and superheavy nuclei.

The use of a schematic interaction makes the theory extremely powerful for practical applications. It is rather amazing that such simple schematic forces can describe a large number of different types of nuclei consistently and accurately. It may imply that they indeed represent the most important parts of the effective nucleon correlations in nuclei, as discussed in Refs.[15,16].

An important shell model application is to provide the structure information and decay rates for nuclear astrophysics. There have been some shell model applications along this line (see, for example, Ref.[4]); however, it still has a very long way to go. A large, unexplored region is the region away from the β-stability, in which nuclear astrophysics is much interested. There are many questions for every shell model, including the PSM, to answer; the immediate ones are those concerning the choice of proper effective interactions and single particle states for the new regions.

Acknowledgements

The author would like to thank the organizers of the 2006 International Conference on Nuclear Structure Physics in Shanghai for inviting him to the conference. He is very grateful to the following people for many discussions and contributions to this paper: A. Aprahamian, Y.-S. Chen, J. Fisker, Z.-C. Gao, M. Guidry, M. Hasegawa, K. Kaneko, G.-L. Long, T. Mizusaki, H. Schatz, P. M. Walker, M. Wiescher, C.-L. Wu, F.-R. Xu, E.-G. Zhao, X.-R. Zhou, as well as R.-D. Herzberg and the ^{254}No experimental collaborators. This work is supported by the National Science Foundation of USA under contract PHY-0140324 and PHY-0216783.

References

1. E. Caurier, G. Martínez-Pinedo, F. Nowacki, A. Poves, and A. P. Zuker, *Rev. Mod. Phys.* **77** (2005) 427.
2. K. Hara and Y. Sun, *Int. J. Mod. Phys.* **E4** (1995) 637.
3. A. Aprahamian, K. Langanke, and M. Wiescher, *Prog. Part. Nucl. Phys.* **54** (2005) 535.
4. K. Langanke and G. Martínez-Pinedo, *Rev. Mod. Phys.* **75** (2003) 819.
5. F. Iachello and A. Arima, *The Interacting Boson Model* (Cambridge University Press, Cambridge, 1987).
6. C.-L. Wu, D. H. Feng, and M. W. Guidry, *Adv. Nucl. Phys.* **21** (1994) 227.
7. G. Popa, J. G. Hirsch, and J. P. Draayer, *Phys. Rev.* **C62** (2000) 064313.
8. Y. M. Zhao, N. Yoshinaga, S. Yamaji, J. Q. Chen, and A. Arima, *Phys. Rev.* **C62** (2000) 014304.
9. K. W. Schmid, *Prog. Part. Nucl. Phys.* **52** (2004) 565.
10. T. Otsuka, M. Honma, T. Mizusaki, N. Shimizu, and Y. Utsuno, *Prog. Part. Nucl. Phys.* **47** (2001) 319.
11. S. G. Nilsson *et al.*, *Nucl. Phys.* **A131** (1969) 1.
12. P. Ring and P. Schuck, *The Nuclear Many Body Problem* (Springer-Verlag, New York, 1980).
13. K. Hara and S. Iwasaki, *Nucl. Phys.* **A332** (1979) 61; **A348** (1980) 200.
14. Y. Sun and K. Hara, *Comput. Phys. Commun.* **104** (1997) 245.
15. M. Dufour and A.P. Zuker, *Phys. Rev.* **C54** (1996) 1641.
16. M. Hasegawa and K. Kaneko, *Phys. Rev.* **C59** (1999) 1449.
17. E. Caurier et al., *Phys. Rev. Lett.* **75** (1995) 2466.
18. K. Hara, Y. Sun, and T. Mizusaki, *Phys. Rev. Lett.* **83** (1999) 1922.
19. G.-L. Long and Y. Sun, *Phys. Rev.* **C63** (2001) 021305(R).
20. C. E. Svensson *et al.*, *Phys. Rev. Lett.* **85** (2000) 2693.
21. P. M. Walker and G. D. Dracoulis, *Nature* **399** (1999) 35.
22. A. Aprahamian and Y. Sun, *Nat. Phys.* **1** (2005) 81.
23. G. C. Baldwin and J.C. Solem, *Rev. Mod. Phys.* **69** (1997) 1085.
24. S. M. Mullins *et al.*, *Phys. Lett.* **B393** (1997) 279; **B400** (1997) 401.
25. A. B. Hayes *et al.*, *Phys. Rev. Lett.* **89** (2002) 242501.
26. Y. Sun, X.-R. Zhou, G.-L. Long, E.-G. Zhao, and P. M. Walker, *Phys. Lett.* **B589** (2004) 83.
27. F. R. Xu, E. G. Zhao, R. Wyss, and P. M. Walker, *Phys. Rev. Lett.* **92** (2004) 252501.
28. R.-D. Herzberg *et al.*, *Nature* **442** (2006) 896.
29. H. Schatz *et al.*, *Phys. Rep.* **294** (1998) 167.
30. Y. Sun, M. Wiescher, A. Aprahamian, and J. Fisker, *Nucl. Phys.* **A758** (2005) 765.
31. Y. Sun, *Eur. Phys. J.* **A20** (2004) 133.
32. E. Bouchez *et al.*, *Phys. Rev. Lett.* **90** (2003) 082502.
33. K. Kaneko, M. Hasegawa, and T. Mizusaki, *Phys. Rev.* **C70** (2004) 051301(R).
34. J. L. Fisker, E. Brown, M. Liebendörfer, H. Schatz, and F.-K. Thielemann, *Nucl. Phys.* **A758** (2005) 447.
35. B. H. Wildenthal, Prog. Part. Nucl. Phys. **11**, 5 (1984).
36. B. A. Brown and B. H. Wildenthal, At. Data Nucl. Data Tables **33**, 347 (1985).
37. T. Oda, M. Hino, K. Muto, M. Takahara, and K. Sato, At. Data Nucl. Data Tables **56**, 231 (1994).
38. K. Langanke and G. Martínez-Pinedo, At. Data Nucl. Data Tables **79**, 1 (2001).
39. Z. C. Gao, Y. Sun, and Y. S. Chen, *Phys. Rev.* **C**, to be published.